

# A Model for Predicting the Power Delay Profile Characteristics Inside a Room

Christopher L. Holloway, *Member, IEEE*, Michael G. Cotton, *Member, IEEE*, and Paul McKenna, *Member, IEEE*

**Abstract**—Multipath effects in indoor wireless communication systems exhibit a characteristic power delay profile (PDP) and can be a detriment to system performance. In this paper, we present a simplified model for calculating the decay rate of the PDP for propagation within rooms. This simplified model provides a time-efficient means of predicting system performance. Predictions of this in-room PDP model are compared to results obtained from a finite-difference time-domain (FDTD) model. Additionally, comparisons of the IPDP model to measured data are presented. The rms delay spread is the second central moment of the PDP of a propagation channel and is a measure of the communication link degradation due to multipath. We also show results of the estimated rms delay spread from this model and show comparisons to the measured data. This IPDP model can be used to investigate the effects of variable room size and properties of the surfaces (or walls) on the decay characteristics of the PDP.

**Index Terms**—Channel modeling, delay spread, impulse response, multipath, power delay profile.

## I. INTRODUCTION

IN DESIGNING wireless telecommunication systems, it is crucial to control the intersymbol interference (ISI) and more importantly the bit error rate (BER). The ISI is directly related to the multipath phenomena resulting from objects (such as walls, furniture, and people) in the propagation path between the transmitter and receiver. This multipath exhibits a characteristic power delay profile (PDP). The delay spread of the radio propagation channel is a measure of the PDP which can be a detriment to system performance [1]–[10].

While techniques such as equalization [11], [12] and diversity [13]–[15] are often used to mitigate the effects of multipath, it is still important to be able to predict the multipath effects by estimating the impulse response and decay rates in the indoor channel before designing a particular system. There are various techniques available for predicting these multipath effects. Geometric optics (or ray tracing) models [16]–[29], finite-difference time-domain (FDTD) models [30]–[33], and time-domain integral equation models [34] have been used to calculate the impulse response and the PDP for indoor channels. While these numerical techniques are accurate, they are time consuming. Statistical models for indoor radio propagation have also been developed for determining the impulse response [35]–[44]; however, these models are only valid as long as the defining statistics for the channel being modeled are accurate.

In this paper, we introduce a simplified model for calculating the PDP for inside a room. Parameters in this model are functions only of the volume of the room, the surface area of the room, and the amount of energy absorbed into the walls. The predictions from this in-room PDP model are compared to numerical results obtained from a FDTD model, as well as to measured data.

## II. BACKGROUND

Dating back to the turn of the century, the acoustic community has been estimating the decay rates (or reverberation time) of energy inside acoustic cavities (or rooms) [45], [55]. Reverberation of a room occurs when multiple wall reflections are present [56]. Under this condition, the field levels in an acoustic cavity are assumed to be uniform, and the gross tendency of the average energy  $W$  in the room resembles an exponential decay

$$W(t) = W_o \exp(-t/\tau). \quad (1)$$

The expression is usually referred to as the Sabine reverberation equation [48], where  $\tau$  is the characteristic decay time and is given by

$$\tau = \frac{4V}{vS\alpha} \quad (2)$$

where  $V$  is the volume of the room,  $S$  is the surface area of the walls in the rooms,  $v$  is the speed which energy propagates in the room (for acoustic rooms, this is the speed of sound), and  $\alpha$  is the acoustic absorption coefficient defined in [57] and [58].

This approach has been used to calculate the characteristic decay times and the  $Q$  of the acoustic cavity (defined as  $Q = \omega\tau$ ) and for electromagnetic reverberation chambers [59]–[64]. The dissipated energy in the highly conducting walls of these reverberation chambers has been determined by averaging over the individual cavity modes [60] and [63] and by averaging plane wave losses due to reflections over all possible angles of incidence and polarizations [62] and [65]. The latter approach will be utilized in this paper to approximate the power dissipated and reflected by the surfaces (or walls) in rooms.

The above approach for determining the decay time of reverberation rooms, works very well as long as the absorption coefficient  $\alpha$  is small. As  $\alpha$  approaches one, however, the decay time predicted by the Sabine reverberation equation does not approach zero; it approaches a constant. The dilemma of nonzero decay time for rooms with perfectly absorbing walls

Manuscript received December 9, 1997; revised April 2, 1998.

The authors are with the Institute for Telecommunication Sciences, U.S. Department of Commerce, Boulder Laboratories, Boulder, CO 80303 USA.

Publisher Item Identifier S 0018-9545(99)05718-7.

was investigated by researchers analyzing room acoustics in the 1930's and 1940's [49]–[52]. A remedy was proposed by Eyring [49] where he approximated the characteristic decay time of these so-called “dead” rooms as

$$\tau = \frac{l_c}{-v \ln(1 - \alpha)}. \quad (3)$$

The parameter  $l_c$  is defined as the mean-free path between reflections, and for a rectangular room is given by [54], [55], and [66]–[68]

$$l_c = \frac{4V}{S}. \quad (4)$$

This quantity is not the average distance between reflections for any given ray in the room; instead it is  $v$  times the reciprocal of the average reflection frequency (the average number of wall reflections per second). Note that the characteristic decay time given by Sabine [see (2)] and Eyring [see (3)] approaches the same value for small values of  $\alpha$ . Recently, this so-called “dead” room formulation was used to analyze electromagnetic anechoic test chambers [69].

The “live” and “dead” room expressions given in this section are valid as long as reverberation is present in the room. Dunens and Lambert [56] have suggested that reverberation occurs when several wall reflections are present, and more importantly, they have shown that reverberation occurs after  $8l_c/v$  to  $10l_c/v$  s. For indoor wireless communications in rooms where the walls are not highly reflecting, energy propagates freely through walls of typical building materials, and as a result, few wall reflections occur. Before  $10l_c/c$  s elapses (where  $c$  is the speed of propagation of electromagnetic waves), only a minimal amount of energy is left in the room. The situation when few wall reflections are present in a cavity is referred to as a nonreverberated regime.

The study of acoustics concentrates primarily in units of energy. In wireless communication applications, however, the way in which the power level in a room decays with time (i.e., the PDP) is more important. By extending the concept presented in this section, it is possible to derive an expression for the average PDP of a room when relatively few wall reflections are present.

### III. IN-ROOM PDP MODEL

In developing the decay time for “dead” rooms in acoustics, Eyring assumed discontinuous drops in the power levels caused by wall reflections [49] and [55]. Using these same concepts, we developed an in-room PDP model. If an electromagnetic pulse is launched from a transmitter at some location, the received power at some other location in the room is depicted by Fig. 1. After some time delay  $t_o$ , from the time the pulse leaves the transmitter, the power in the direct ray arrives at the receiver. The power level in the direct ray is usually the strongest signal and the time delay is given by  $t_o = d/c$ , where  $d$  is the separation distance of the receiver and transmitter and  $c$  the speed of electromagnetic propagation in the room. This direct ray is illustrated by the thick arrow in Fig. 1. The strength of this direct ray is  $P_o$ .

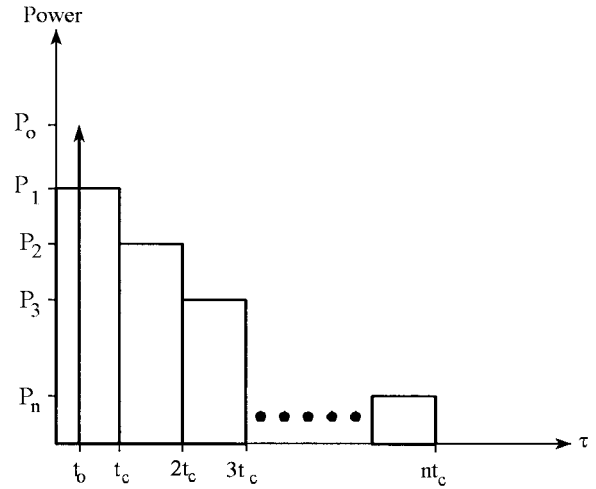


Fig. 1. Typical field level distribution inside a room.

All the delayed components are due to reflections or scattering from objects such as walls, floor, ceiling, furniture, and people in the propagation path between the transmitter and receiver. To simplify this analysis, assume that the room is empty, such that all reflection originates from only the ceiling, floor, and walls. On average, after some given time delay  $t_c$ , all the pulses that make only one reflection off either the ceiling, floor, or walls, will arrive at the receiver. This time delay  $t_c$  is defined as the characteristic room time, and is formulated below. Pulses that arrive at the receiver after only one reflection have some mean power level  $P_1$ . This power level is decreased from the transmitted power level by two primary attenuation factors. The first is simply the free-space loss proportional to  $1/r^2$ , where  $r$  is the path length that these rays travel. The second is the reduction in power due to reflection and absorption characteristics of the surfaces in the room. All pulses arriving after one reflection are represented in Fig. 1 by the rectangular box with height  $P_1$  and width  $t_c$ .

After some other time delay, or two characteristic times  $2t_c$ , it is assumed that all pulses arriving at the receiver would have made only two reflections. Pulses that arrive at the receiver after two reflections have some mean power level  $P_2$ . This power level is a function of the path length and the reflection coefficient of two reflecting surfaces. It is assumed, on average, that pulses making two bounces will not arrive at the receiver until most of the pulses that make only one reflection have arrived. The rectangular box with height  $P_2$  and width  $t_c$  in Fig. 1 represents the pulses that arrive after two reflections. This process continues for additional reflections until the power levels are negligible. The series of rectangles in Fig. 1 represents the pulses arriving at the receiver after  $n$  reflections with power levels given by  $P_n$ . As discussed below, the PDP is approximated by connecting the direct ray and the tops of the rectangular boxes representing the multipath components.

#### A. Characteristic Time $t_c$ of a Room

The acoustic community uses the mean-free path  $l_c$  as a means to determine characteristics about a room response.

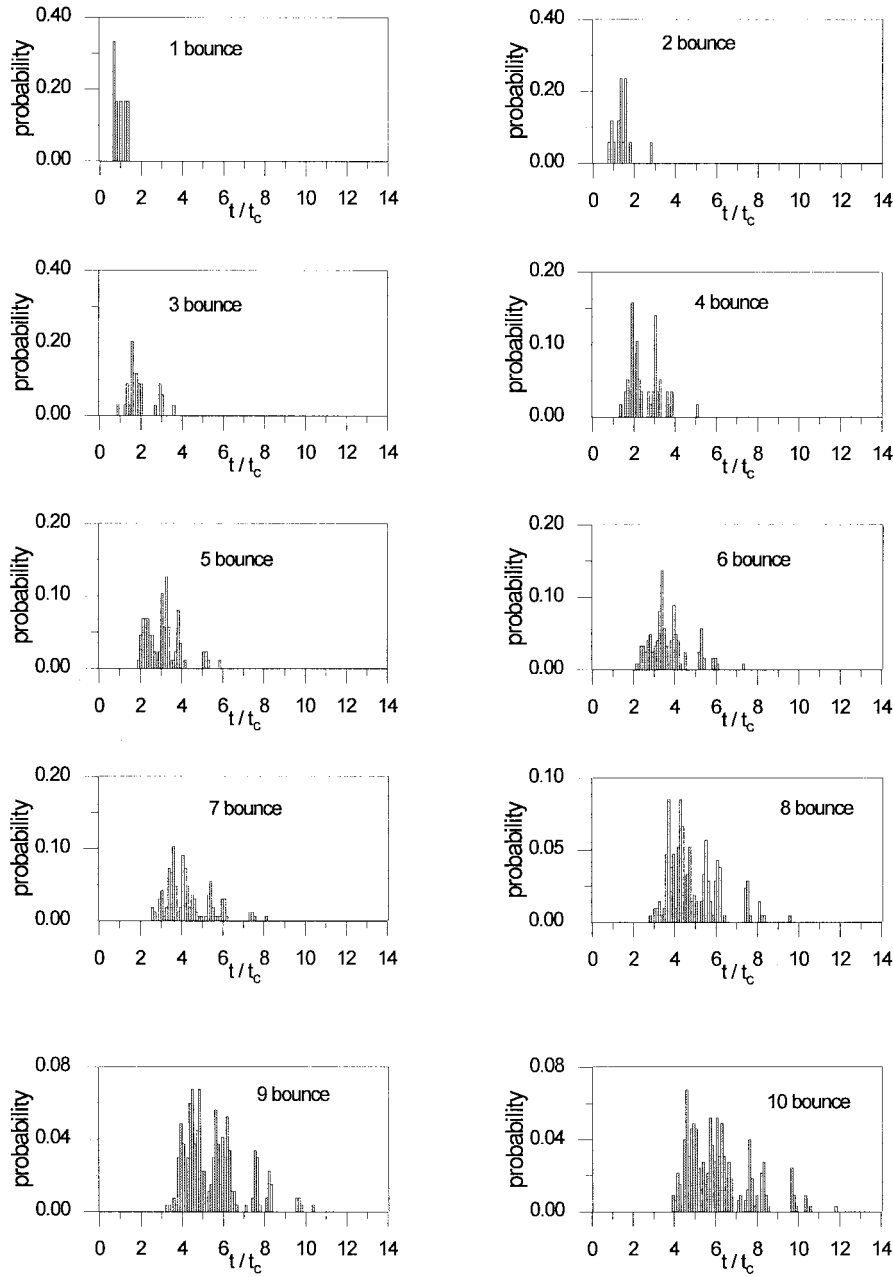


Fig. 2. Histograms of travel times of rays making  $n$  bounces.

Actually, the quantity  $l_c/v$  is used as a means of estimating transience in a given room size. The characteristic time  $t_c$  of a room that is required before a given set of rays makes one reflection is assumed to be given by a function of the mean-free path  $l_c$  and by utilizing (4) can be expressed as

$$t_c = 2 \frac{l_c}{c} = \frac{8V}{cS}. \quad (5)$$

The justification of representing the characteristic time  $t_c$  in this manner is illustrated in Fig. 2. Using a ray trace model, the arrival times were determined for rays making  $n$  bounces from the ceiling, floor, and walls in a room with a length of 6 m, height of 3 m, and width of 4 m. Probability distribution curves versus arrival times for rays making  $n$  bounces are shown. The first plot corresponds to the distribution of arrival times

for rays making only one bounce in the room. The remaining plots in Fig. 2 correspond to the distribution of arrival times for rays making two–ten bounces, respectively. Notice if a ray makes  $n$  bounces off reflecting surfaces, then by  $t = nt_c$ , the majority of the  $n$ -bounced rays have arrived at the receiver. That is to say, by  $t = t_c$ , most of the rays making one bounce arrive at the receiver; by  $t = 2t_c$ , most of the rays making two bounces arrive at the receiver, and so on for increasing number of bounces.

### B. Reflected Power Levels

In both electromagnetic and acoustic reverberation rooms, the decay rate of energy is a function of the energy dissipated into the walls, floor, and ceiling through the parameter  $\alpha$

[45], [55], [59]–[65], and [69]). The path length the rays travel is unimportant in the energy levels of reverberation cavities, because reverberation assumes the energy is uniformly distributed throughout the cavity. The model presented here attempts to predict the PDP for a situation where the room is not reverberant. In fact, for most in-room wireless communication applications, the energy in the room will dissipate quickly and the reverberation conditions are rarely met. For this type of scenario, the power levels will be a function of the path lengths the rays travel, as well as the power dissipated in the reflecting surfaces.

It is possible to determine the path length and reflection coefficient of each ray striking a surface in a room using ray tracing approaches [16]–[29]. However, this approach as well as other numerical approaches [30]–[34] are time consuming. By using characteristic parameters of a room, it is possible to approximate the power levels at different times. The average power level of the bundle of rays that correspond to rays after  $n$  reflections is approximated by

$$P_n = A \frac{\gamma^n}{d_n^2}. \quad (6)$$

$A$  is a constant that is a function of the transmitting and receiving antennas and the transmitted power, and  $d_n$  is the characteristic or effective distance that a bundle of rays making  $n$  reflections travels and is approximated by the time it takes these rays to reach the receiver (that is, some integer multiple of the characteristic time  $t_c$ ). Using the definition of  $t_c$  given in (5),  $d_n$  is expressed in terms of the characteristic length or mean-free path  $l_c$  as

$$d_n = nt_c c = 2nl_c. \quad (7)$$

In (6),  $\gamma$  is the average power reflection coefficient. In general, it would be involved to determine the reflection coefficient from the incident angle and polarization of each ray in the room. Since we are only interested in the reflected power in an average sense, the average power reflection coefficient can be calculated in the same manner as is done in electromagnetic reverberation rooms [65] and [69]. Thus, the average power reflection coefficient is defined as

$$\gamma = 1 - \alpha \quad (8)$$

where  $\alpha$  is the average absorption coefficient of the surfaces in the rooms. It is calculated by averaging plane-wave reflection coefficients over all possible angles of incidence and polarizations [65] and [69] and is expressed as

$$\alpha = 2 \int_0^{\pi/2} \left\{ 1 - \left[ \frac{|R_{TM}(\theta)|^2 + |R_{TE}(\theta)|^2}{2} \right] \right\} \cdot \sin \theta \cos \theta d\theta \quad (9)$$

where  $R_{TE}(\theta)$  and  $R_{TM}(\theta)$  are the plane-wave reflection coefficients for transverse electric and transverse magnetic waves, respectively. The plane-wave reflection coefficients are functions of the material properties, thickness of the reflection surfaces, and frequency of operation. Expressions for  $R_{TM}(\theta)$  and  $R_{TE}(\theta)$  can be found in [70] and [71].

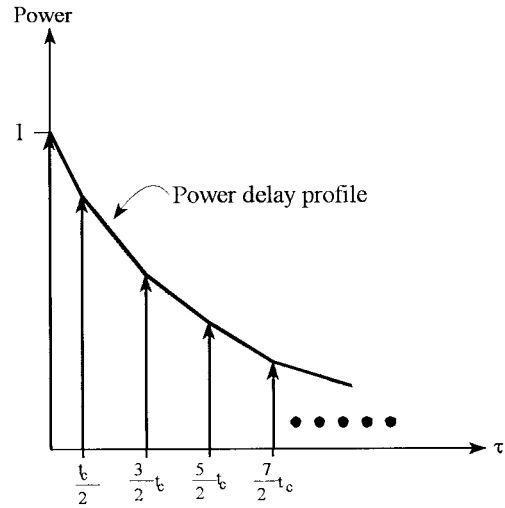


Fig. 3. Normalized PDP model for an in-room wireless radio propagation channel.

### C. Direct Ray

The direct ray arrives at the receiver at a time delay determined by the transmitter and receiver antenna separation  $d_o$ . The power level of the direct ray at the receiver is given by

$$P_o = \frac{A}{d_o^2} \quad (10)$$

where  $A$  is a constant. The antenna separation distance is known for a specific configuration, but the goal of this analysis is to determine the PDP of the room in an average sense, that is, to determine the global behavior of the room without knowing the exact location of the transmitter and receiver, or to determine the room average performance. Thus, it is assumed that on average, the direct path travels a distance equal to one characteristic length of the room  $d_o = l_c$  and the direct ray arrives at the receiver at  $t = t_o = l_c/c$ .

### D. Power Delay Profile

With the power level and delay times of the direct ray and the reflected rays determined, the PDP can be modeled. By initializing the delay time of the direct ray to zero and normalizing the power to  $P_o$ , the power levels at different delay times are approximated by

$$\begin{aligned} \text{PDP}_o &= 1 \quad \tau = 0, \quad \text{for } n = 0 \\ \text{PDP}_n &= \frac{1}{4} \frac{\gamma^n}{n^2}, \quad \tau_n = \frac{t_c}{2}(2n - 1), \quad \text{for } n \neq 0. \end{aligned} \quad (11)$$

This normalized PDP is depicted in Fig. 3. By connecting the arrows in this figure, an approximation to the PDP is obtained. One needs to keep in mind that this PDP is not for a particular location in a room; it corresponds to the average room behavior.

### E. Room Consisting of Different Reflecting Surfaces

The average reflected power calculated from (8) assumes that all the reflecting surfaces are identical. When different reflecting surfaces are present in a room the average power reflection coefficient is calculated as a weighted average of

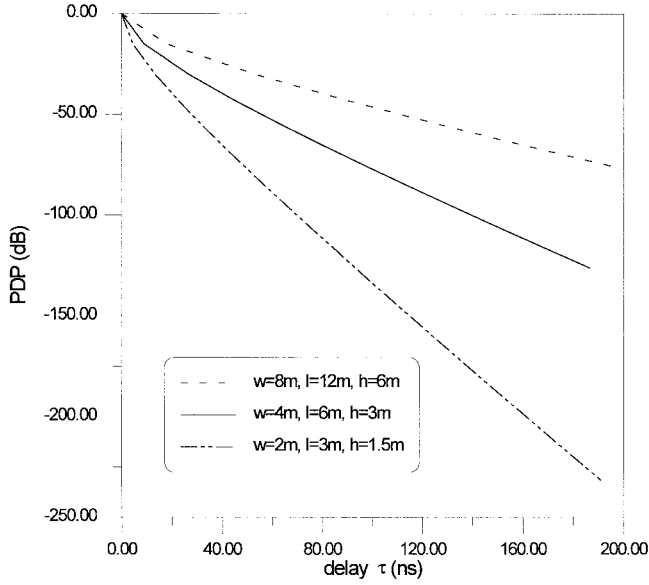


Fig. 4. Variations of the PDP for different size rooms.

all the surfaces, similar to what is done in acoustic and electromagnetic cavities [49] and [69]. The effective average absorption and the consequent average power reflection coefficient in a room with different reflecting surfaces is given by

$$\alpha_{\text{eff}} = \frac{\sum S_n \alpha_n}{S} \quad (12)$$

$$\gamma_{\text{eff}} = 1 - \alpha_{\text{eff}}$$

where  $S$  is the total surface area of the room,  $S_n$  is the area of surface  $n$ , and  $\alpha_n$  is the average absorption of surface  $n$ .

#### IV. GEOMETRY AND MATERIAL PROPERTIES VARIATIONS

The IPDP model was implemented to investigate the effects of variable room size and properties of the surfaces (or walls) on the PDP. The first example illustrates the effects of room size. Fig. 4 shows the PDP for a room 4 m wide, 3 m high, and 6 m long. The surfaces (walls, ceiling, and floor) in this room are composed of an infinitely thick homogenous concrete slab with  $\epsilon_r = 3$  and  $\sigma = 0.01$  S/m. Also shown in this figure are results for the same surfaces with the dimensions of the room doubled and halved. These results are obtained for a frequency of 1.5 GHz. For all three of these rooms, the average absorption and reflection coefficients of the surfaces are  $\alpha = 0.88$  and  $\gamma = 0.12$ . These results illustrate, as one might expect, that for the large room, the energy rings longer. This results in the power levels remaining relatively high for long periods of time. For the smallest room dimension, the power levels decay relatively quickly.

The effects of different material properties of the surfaces were also investigated. Fig. 5 shows the PDP for a room 4 m wide, 3 m high, and 6 m long. The surfaces in this room are assumed to be infinitely thick and homogenous with  $\epsilon_r = 3$  and  $\sigma = 0.01$  S/m ( $\alpha = 0.88$  and  $\gamma = 0.12$ ). Also shown in this figure are results for the same room size with the conductivities increased to  $\sigma = 0.1$  S/m ( $\alpha = 0.86$  and

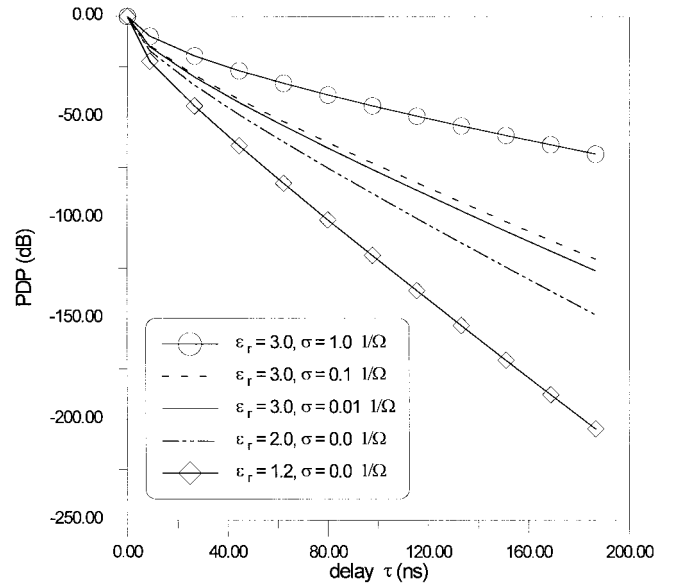


Fig. 5. Variations of the PDP for a room 4 m wide, 3 m high, and 6 m long for different types of wall materials.

$\gamma = 0.14$ ) and  $\sigma = 1.0$  S/m ( $\alpha = 0.58$  and  $\gamma = 0.42$ ). Other results shown in this figure are for the same size room with  $\epsilon_r = 2$  and  $\sigma = 0.0$  S/m ( $\alpha = 0.92$  and  $\gamma = 0.08$ ) and  $\epsilon_r = 1.2$  and  $\sigma = 0.0$  S/m ( $\alpha = 0.98$  and  $\gamma = 0.02$ ). When the reflections from the surfaces are large, the field strength in the room remains relatively high for long periods of time, illustrated by  $\sigma = 1.0$  S/m ( $\alpha = 0.58$  and  $\gamma = 0.42$ ). On the other hand, when the reflections from the surfaces are small, the field strength in the room will decay relatively quickly in a short period of time, illustrated by  $\epsilon_r = 1.2$  and  $\sigma = 0.0$  S/m ( $\alpha = 0.98$  and  $\gamma = 0.02$ ).

Finally, the effect of surfaces consisting of different materials was investigated. In the three examples investigated, it was assumed that the material properties of the ceiling are different from the other reflecting surfaces in the room. For this condition, the effective absorption coefficient given by (12) reduces to the following for a room for the two types of reflecting surfaces:

$$\alpha_{\text{eff}} = \alpha_{w,f} \frac{S - S_c}{S} + \alpha_c \frac{S_c}{S} \quad (13)$$

where  $S$  is the total surface area of the room,  $S_c$  is the surface area of the ceiling,  $\alpha_c$  is the average absorption coefficient of the ceiling, and  $\alpha_{w,f}$  is the average absorption coefficient of the walls and floor. In the first example, it was assumed that all the reflecting surfaces (including the walls, floor and ceiling) are composed of the same material ( $\epsilon_r = 3$  and  $\sigma = 0.01$  S/m) and are of infinite thickness. When all the surfaces in the room are the same, the average absorption and reflection for the room can be calculated by (8) and (9) and are  $\alpha_{w,f,c} = 0.88$  and  $\gamma_{w,f,c} = 0.12$ . In the second example, it was assumed that the ceiling of the room is perfectly absorbing (i.e.,  $\alpha_c = 1.0$  and  $\gamma_c = 0.0$ ) and the walls and floor have the same material as in the first example (i.e.,  $\alpha_{w,f} = 0.88$  and  $\gamma_{w,f} = 0.12$ ). The last example corresponds to a room with a ceiling that is perfectly reflecting (i.e.,  $\alpha_c = 0.0$  and  $\gamma_c = 1.0$ ) and the

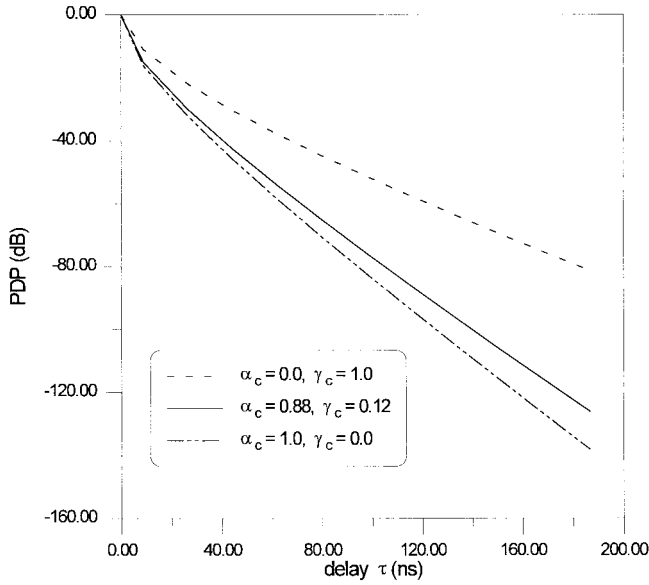


Fig. 6. Variations of the PDP for a room with different materials in the ceiling.

walls and floor have the same material as in the first example (i.e.,  $\alpha_{w,f} = 0.88$  and  $\gamma_{w,f} = 0.12$ ). The results of all three of these examples are shown in Fig. 6. This figure illustrates how the field levels in a room vary as the properties of one of the reflecting surfaces in a room change. As expected, as  $\gamma_{\text{eff}}$  increases, the power levels in the room remain at relatively high levels for longer periods of time.

## V. WIDE-BAND SYSTEMS

The IPDP model presented here has a frequency dependence due to the average reflected power being a function of the reflection coefficient of the reflecting surfaces. These reflection coefficients are functions of the material properties, surface (or wall) thickness, and frequency. The question that arises is: what frequency should be used when a system has a given bandwidth? Fig. 7 shows results of  $\gamma$  for different types of surfaces at various frequencies. If  $\gamma$  does not vary appreciably in the given bandwidth, then the value of  $\gamma$  at the carrier frequency can be used. However, for some materials and wall geometries,  $\gamma$  can exhibit a strong resonant behavior in a given bandwidth of frequencies (see the solid curve in Fig. 7). By using the maximum average reflected power  $\gamma_{\text{max}}$  in the given bandwidth in our IPDP model, a worst case or upper limit on the decay rate is obtained since the IPDP model is directly related to the value of  $\gamma$ . Thus, to calculate the PDP for a wide-bandwidth system,  $\gamma$  is calculated for the entire bandwidth and the maximum average reflected power  $\gamma_{\text{max}}$  is used.

The question whether distortion due to variation of the  $\gamma$  in the whole band is significant will depend on the resonant behavior of  $\gamma$  (which is a function of materials and geometry of the walls). Part of our future work in developing and improving this model is to investigate this issue.

## VI. VALIDATION OF THE MODEL

We validated the PDP model by comparing it to results obtained from a FDTD model and measured data. We are

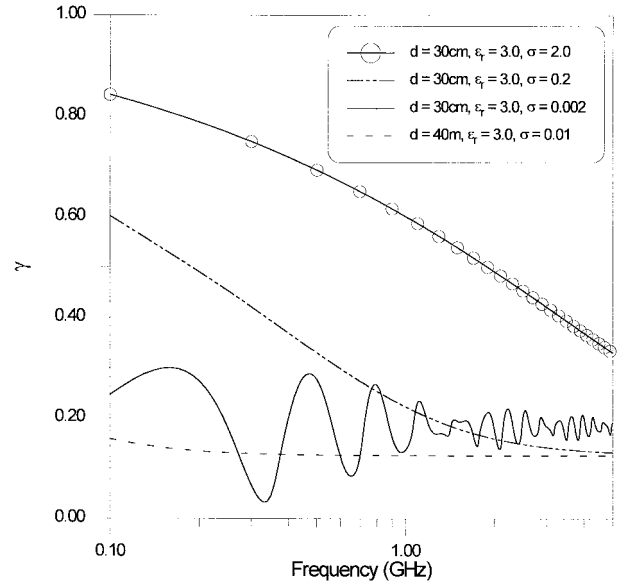


Fig. 7. Variations of  $\gamma$  for a room with different types of reflecting surfaces.

investigating the use of a three-dimensional (3-D) FDTD approximation to Maxwell's curl equations to determine the impulse response of the in-room channel. The FDTD technique requires the volume of the room and the walls to be subdivided into unit cubic cells. The electric and magnetic field vector components on these cells are represented by a Yee space lattice [72]. With this space lattice, the Yee algorithms ([72] and [73]) for the coupled Maxwell's curl equations can be used to solve for both the electric and magnetic fields in time and space. The finite-difference grid was continued three spatial cells beyond the outer edges of the walls, and the grid was terminated at that point by an absorbing boundary condition. A 16-cell-thick Berenger perfectly matched layer with a quadratic conductive profile was used as the absorbing boundary condition [74].

Fig. 8 shows the results of predicted PDP's for two different locations in a room obtained from the FDTD simulation. The current source waveform used in this simulation corresponded to a first derivative of a Gaussian. The results in the figure correspond to a room 2.4 m high, 3.3 m wide, and 5.4 m long and the walls, floor, and ceiling for this room have a thickness of 30 cm with  $\epsilon_r = 3.0$  and  $\sigma = 0.01$  S/m. Also shown in this figure are corresponding results from the IPDP model. Fig. 9 shows a comparison of the IPDP model and the FDTD model for a room with the same dimensions and with the conductivity increased to 2.0 S/m. The comparisons in these two figures illustrate that the IPDP model predicts the same decay characteristics in the PDP as predicted from the FDTD model.

Finally, comparisons to measured data are presented. Our Institute has developed an impulse measurement system to measure the PDP for an in-room propagation channel. This system is based on a correlation technique using a pseudorandom transmitted code and is detailed in [75] and [76]. This system measures a bandlimited impulse response at a carrier frequency of 1.5 GHz with bandwidth of 500 MHz. The PDP was measured in two different rooms. The first room is a small

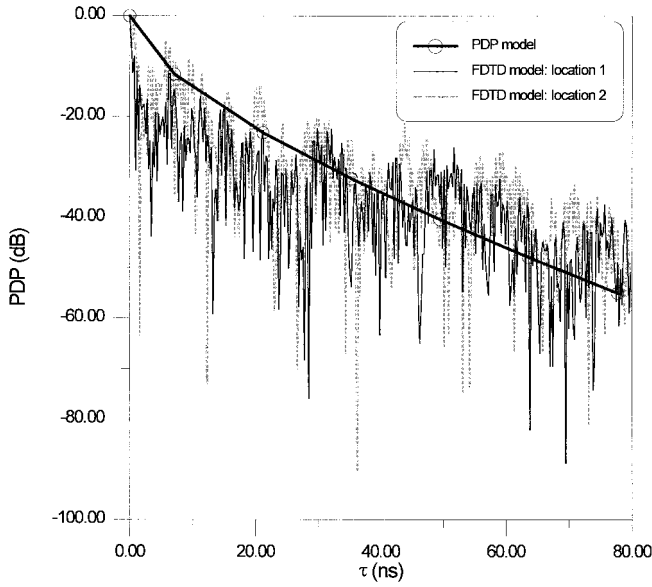


Fig. 8. Comparison of the IPDP model to the FDTD simulation for a room with a length of 5.4 m, a width of 3.3 m, and a height of 2.4 m, assuming the walls are 30 cm thick with  $\epsilon_r = 3.0$  and  $\sigma = 0.01$  S/m.

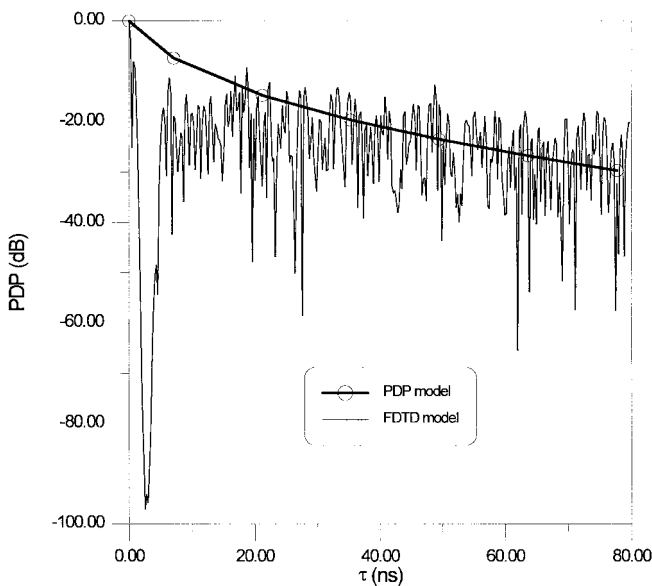


Fig. 9. Comparison of the IPDP model to the FDTD simulation for a room with a length of 5.4 m, a width of 3.3 m, and a height of 2.4 m, assuming the walls are 30 cm thick with  $\epsilon_r = 3.0$  and  $\sigma = 2.0$  S/m.

office with a height of 3.20 m, a width of 2.31 m, and a length of 5.26 m. The second room is a laboratory with a height of 5.0 m, a width of 7.18 m, and a length of 9.35 m. The walls in the office and laboratory were composed of concrete slabs and concrete blocks of thickness 14.5 cm with  $\epsilon_r = 6.0$  and  $\sigma = 1.95 \cdot 10^{-3}$  S/m [77].

Figs. 10 and 11 show comparisons of the IPDP model to measured data for these two rooms. The measured data in both rooms were obtained with the transmitter located near a corner of their respective room at a height of 1.8 m and the receiver was placed on a cart with an antenna height of 1.8 m. Location 1 in Figs. 10 and 11 corresponds to the receiver placed at a location near one of the walls of the respective

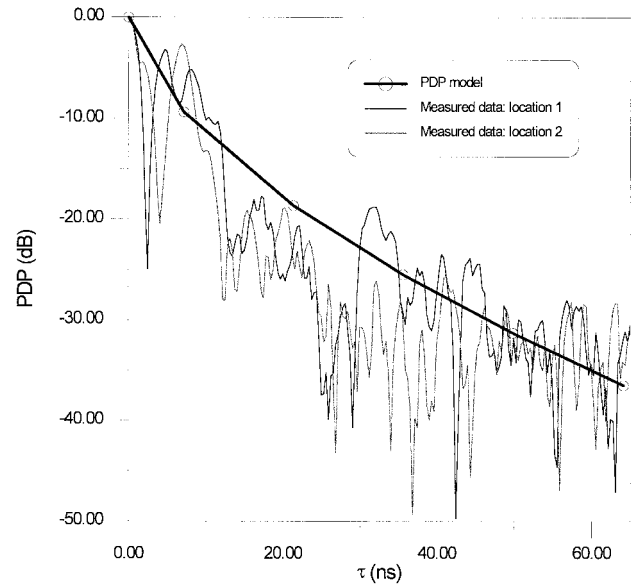


Fig. 10. Comparison of the IPDP model to measured data for a small office with a length of 5.26 m, a width of 2.31 m, and a height of 3.20 m.

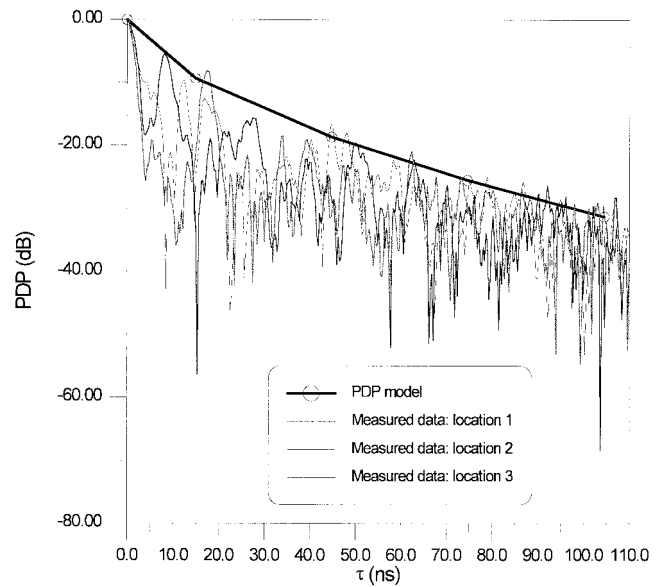


Fig. 11. Comparison of the IPDP model to measured data for a laboratory with a length of 9.35 m, a width of 7.18 m, and a height of 5.00 m.

rooms, and Location 2 in the two figures corresponds to the receiver placed at the center of the respective rooms. Location 3 in Fig. 11 corresponds to the transmitter being placed at the center of the laboratory and the receiver placed 2 m from one of the walls. The comparisons in these two figures illustrate that the IPDP model predicts the same decay characteristics in the PDP as seen in the measurements.

With the receiver placed on a moveable cart, the impulse responses for several locations distributed throughout the rooms were obtained. The magnitude of all of the impulse responses in each of the two rooms were averaged together to obtain an effective average PDP of each room. The results of these averages along with the results of the IPDP model are shown in Figs. 12 and 13 for the office and laboratory,

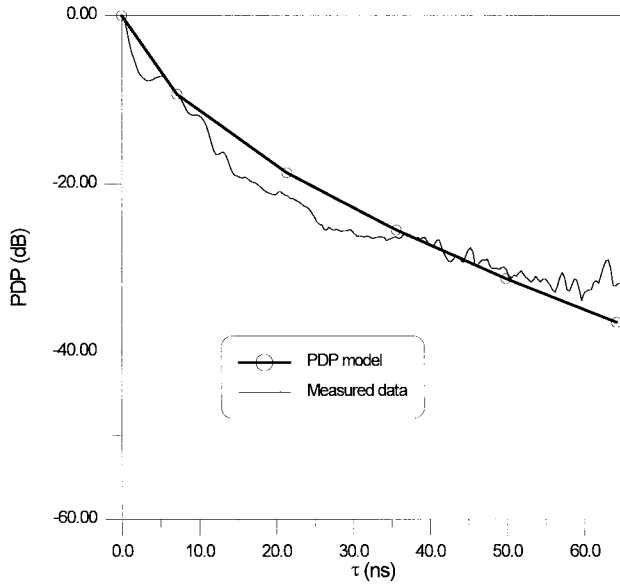


Fig. 12. Comparison of the IPDP model to the measured data obtained by averaging several locations through the office with a length of 5.26 m, a width of 2.31 m, and a height of 3.20 m.

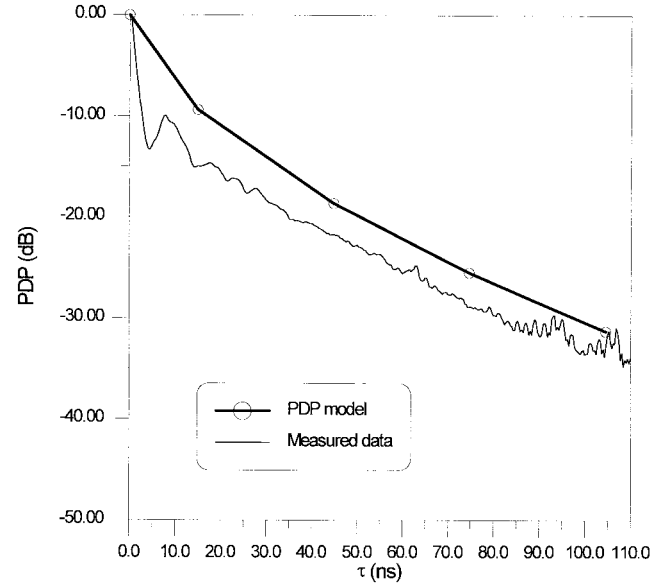


Fig. 13. Comparison of the IPDP model to the measured data obtained by averaging several locations through the laboratory with a length of 9.35 m, a width of 7.18 m, and a height of 5.00 m.

respectively. The comparisons in these two figures illustrate once again that the IPDP model predicts the same decay characteristics in the PDP as seen in the measurements.

The results of the IPDP model can be used to estimate the rms delay spread for these two rooms. The rms delay spread is calculated by the following expression [1] and [4]:

$$\tau_{\text{rms}} = \left[ \frac{\int (t - D)^2 \text{PDP}(t) dt}{\int \text{PDP}(t) dt} \right]^{1/2}$$

where

$$D = \frac{\int t \text{PDP}(t) dt}{\int \text{PDP}(t) dt}.$$

Using the results of our model, we estimated a rms delay spread of 6.1 ns for the office and 13.2 ns for the laboratory. The rms delay spread was also calculated from the measured data. For the office, the rms delay spread for locations 1 and 2 were calculated to be 7.5 and 5.9 ns, respectively. From the measured average PDP of the office (see Fig. 12), the rms delay spread was calculated to be 7.5 ns. For the laboratory, the rms delay spread for locations 1–3 were calculated to be 14.7, 12.5, and 15.1 ns, respectively. From the measured average PDP of the laboratory (see Fig. 13), the rms delay spread was calculated to be 15.6 ns. The rms delay spread obtained from the measured data of the two different rooms compares well to the delay spread obtained from the model. Keeping in mind that the IPDP model in its present form neglects the energy propagation through doors and windows, and scattering and reflections from lights fixtures, air-conditioning units, and piping (which were present in these two rooms), we conclude that the IPDP model agrees well to measured data in predicting the room PDP characteristics.

## VII. DISCUSSION AND CONCLUSION

In this paper, we present a model for predicting the characteristics of the PDP of an in-room wireless propagation channel. This IPDP model is based on simple room parameters: room volume, surface area, and the average power reflected from surfaces in the room. Comparisons to FDTD results and to measured data are presented. From these comparisons it was demonstrated that the IPDP model can be used to predict the decay characteristics of the PDP and estimated the rms delay spread within a room.

The IPDP model does not give a detailed description of a room impulse response. The intent of this model is to give a global (or average) behavior of the channel for the system placed in an arbitrary room location. The advantage of this IPDP model is that it is based on simple assumptions, so the PDP within a room can be calculated in a matter of seconds on a personal computer. Hence, the IPDP model can be used to quickly assess the average response of a room. Furthermore, the IPDP model is a time-efficient means for approximating the rms delay spread and consequent ISI of a specified wireless in-room channel. The IPDP model was used to estimate the rms delay spread and comparison to the measured data show good correlation.

The IPDP model presented here is valid until reverberation occurs in the room. Dunens and Lambert [56] have shown that reverberation occurs after  $8l_c/v$  to  $10l_c/v$  s, which suggests that the model presented here will predict the decay rate of the PDP for times less than five characteristic room times (that is,  $t < 5t_c$ ). For  $t > 5t_c$ , modifications are required for this model to account for room reverberation. For most applications (rooms with highly absorbing walls), the energy in a room decays to minimal levels before reverberation can occur. However, wireless links are being implemented in places with highly conducting walls (i.e., metal warehouses and shipboard communications). Under these types of propagation

environments, the model presented here must be combined with the reverberation decay rate approaches [59]–[64], [69]. The combination of these two approaches is presently being investigated for shipboard communication.

Future work will also include predicting the PDP's of coupled or adjacent rooms and to account for the leakage of energy through doors and windows. Other areas of future work are the effects of furniture in the room and the effects of realistic antenna patterns. It is believed that the effects of narrow beam antenna patterns can be incorporated into the model by weighting the angle dependence of the average reflection given in (9), but this is still being investigated.

While the model presented here is simple to implement, it does require knowing material properties and geometries of the reflecting walls in the room. Until recently [78]–[82], little effort has been given to characterizing building materials. More work in this area is needed, not just for this model, but for all types of indoor field strength prediction models and for impulse response models.

#### ACKNOWLEDGMENT

The authors would like to thank Y. Lo and P. Papazian of the Institute for Telecommunication Sciences for supplying measured impulse response data. They also thank K. C. Allen of the Institute for Telecommunication Sciences and D. A. Hill of the National Institute of Standards and Technology for their helpful discussions.

#### REFERENCES

- [1] J. C. I. Chuang, "The effects of time delay spread on portable radio communication channels with digital modulation," *IEEE J. Select. Areas Commun.*, vol. 5, no. 5, pp. 879–889, 1987.
- [2] P. A. Bello and B. D. Nelin, "The effect of frequency selective fading on the binary error probabilities of incoherent and differentially coherent matched filter receivers," *IEEE Trans. Commun. Syst.*, pp. 170–186, June 1963.
- [3] M. Wittmann, J. Marti, and T. Kürner, "Impact of the power delay profile shape on the bit error rate in mobile radio systems," *IEEE Trans. Veh. Technol.*, vol. 26, no. 2, pp. 329–339, 1997.
- [4] D. M. J. Devasirvatham, "Multipath time delay spread in the digital portable radio environment," *IEEE Commun. Mag.*, vol. 25, no. 6, pp. 13–21, 1987.
- [5] L. J. Greenstein and V. K. Prabhu, "Analysis of multipath outage with applications to 90-Mbits/s PSK systems at 6 and 11 GHz," *IEEE Trans. Commun.*, vol. 27, no. 1, pp. 68–75, 1979.
- [6] R. C. V. Macario, Ed., *Modern Personal Radio Systems*. London, U.K.: IEE, 1996, ch. 3.
- [7] C. A. Siller, Jr., "Multipath propagation," *IEEE Commun. Mag.*, vol. 22, no. 2, pp. 6–15, 1984.
- [8] K. Pahlavan and A. H. Levesque, *Wireless Information Networks*. New York: Wiley, 1995, ch. 8.
- [9] T. S. Rappaport, *Wireless Communications: Principles and Practice*. Upper Saddle River, NJ: Prentice-Hall, 1996, ch. 5.
- [10] W. C. Jakes, "An approximate method to estimate an upper bound on the effect of multipath delay distortion on digital transmission," *IEEE Trans. Commun.*, vol. 27, no. 1, pp. 76–81, 1979.
- [11] S. U. H. Qureshi, "Adaptive equalization," *Proc. IEEE*, vol. 53, pp. 1349–1387, 1985.
- [12] R. Steele, Ed., *Model Radio Communications*. New York: IEEE Press, 1995, chs. 6 and 8.
- [13] W. C. Jakes, Ed., *Microwave Mobile Communications*. New York: IEEE Press, 1993, chs. 5 and 6.
- [14] P. L. Perini and C. L. Holloway, "Angle and space diversity comparisons in different mobile radio environments," *IEEE Trans. Antennas Propagat.*, to be published.
- [15] L. Boithias, *Radio Wave Propagation*. New York: McGraw-Hill, 1987, ch. 6.
- [16] M. C. Lawton and J. P. McGeehan, "The application of GTD and ray launching techniques to channel modeling for cordless radio systems," in *Proc. 42nd IEEE Veh. Technol. Conf.*, Denver, CO, 1992, pp. 125–130.
- [17] A. J. Rustako, Jr., N. Amitary, G. J. Owens, and R. S. Roman, "Radio propagation at microwave frequencies for line-of-sight microcellular mobile and personal communications," *IEEE Trans. Veh. Technol.*, vol. 40, no. 1, pp. 203–210, 1991.
- [18] G. Bronson, K. Pahlavan, and H. Rotthor, "Performance prediction of wireless LAN's based on ray tracing algorithms," in *Proc. PIMRC 93*, Yokohama, Japan, pp. 151–156.
- [19] G. Yang and K. Pahlavan, "Analysis of multicarrier modems in an office environment using 3D ray tracing," in *Proc. IEEE GLOBECOM 94*, San Francisco, CA, pp. 42–46.
- [20] S. Y. Seidel and T. S. Rappaport, "A ray tracing technique to predict path loss and delay spread inside building," in *IEEE GLOBECOM 92*, Orlando, FL, pp. 649–653.
- [21] W. Honcharenko, H. L. Bertoni, J. L. Dailing, J. Qian, and H. D. Yee, "Mechanisms Governing UHF propagation on single floors in modern office buildings," *IEEE Trans. Veh. Technol.*, vol. 41, no. 4, pp. 496–504, 1992.
- [22] T. Holt, K. Pahlavan, and J. F. Lee, "A graphical indoor radio channel simulator using 2D ray tracing," in *Proc. 3rd IEEE Int. Symp. Personal, Indoor and Mobile Radio Commun.*, Boston, MA, 1992, pp. 411–416.
- [23] J. W. McKown and R. L. Hamilton, Jr., "Ray tracing as a design tool for radio networks," *IEEE Network Mag.*, vol. 5, no. 6, pp. 27–30, 1991.
- [24] R. A. Valenzuela, "A ray tracing approach to predicting indoor wireless transmission," in *Proc. IEEE Vehicular Technology Conf.*, Secaucus, NJ, 1993, pp. 214–218.
- [25] U. Dersch, J. Troger, and E. Zollinger, "Multiple reflections of radio waves in a corridor," *IEEE Trans. Antennas Propagat.*, vol. 42, no. 9, pp. 1571–1574, 1994.
- [26] S. H. Chen and S. K. Jeng, "An SBR/image approach to indoor radio wave propagation in indoor environments with metallic furniture," *IEEE Trans. Antennas Propagat.*, vol. 45, no. 1, pp. 98–106, 1997.
- [27] S. Y. Seidel and T. S. Rappaport, "Site-specific propagation prediction for wireless in-building personal communication system design," *IEEE Trans. Veh. Technology*, vol. 43, no. 4, pp. 879–891, 1994.
- [28] S. Y. Tan and H. S. Tan, "Modeling and measurements of channel impulse response for an indoor wireless communication systems," *Proc. Inst. Elect. Eng.*, vol. 142, no. 6, pp. 405–410, 1995.
- [29] P. Kreuzgruber, P. Unterberger, and R. Gahleitner, "A ray splitting model for indoor radio propagation associated with complex geometries," in *Proc. IEEE Vehicular Technology Conf.*, Secaucus, NJ, 1993, pp. 227–230.
- [30] L. Talbi and G. Y. Delisle, "Finite difference time domain characterization of indoor radio propagation," in *Electromagnetic Waves Pier 12, Progress in Electromagnetic Research*, J. A. Kong, Ed. Cambridge, MA: EMW, 1996, pp. 251–275.
- [31] A. Lauer, I. Wolff, A. Bahr, J. Pamp, J. Kunisch, and I. Wolff, "Mutli-mode FDTD simulations of indoor propagation including antenna properties," in *Proc. 1995 IEEE 45th Vehicular Technology Conf.*, Chicago, IL, pp. 454–458.
- [32] C. L. Holloway, M. G. Cotton, and P. McKenna, "A simplified model for calculation the decay rate of the impulse response for an indoor propagation channel," in *Proc. 2nd Annu. Wireless Communications Conf.*, Boulder, CO, 1997, pp. 210–214.
- [33] G. Yang, K. Pahlavan, and J. F. Lee, "A 3D propagation model with polarization characteristics in indoor radio channels," in *Proc. IEEE GLOBECOM 93*, Houston, TX, pp. 1252–1256.
- [34] L. Talbi and G. Delisle, "Wideband propagation measurements and modeling at millimeter wave frequencies," in *Proc. IEEE GLOBECOM 94*, San Francisco, CA, vol. 1, pp. 47–51.
- [35] A. A. M. Saleh and R. A. Valenzuela, "A statistical model for indoor multipath propagation," *IEEE J. Select. Areas Commun.*, vol. 5, no. 2, pp. 128–137, 1987.
- [36] D. Moltdar, "Review on radio propagation into and within buildings," *Proc. Inst. Elect. Eng.*, vol. 138, pt. H, no. 1, pp. 61–73, 1991.
- [37] R. Ganesh and K. Pahlavan, "Modeling of the indoor radio channel," *Proc. Inst. Elect. Eng.*, vol. 139, pt. I, no. 5, pp. 153–161, 1991.
- [38] ———, "Statistics of short time and spatial variations measured in wideband indoor radio channels," *Proc. Inst. Elect. Eng.*, vol. 140, pt. H, no. 4, pp. 297–302, 1993.

- [39] T. S. Rappaport, S. Y. Seidel, and K. Takamizawa, "Statistical channel impulse response models for factory and open plan building radio communication system design," *IEEE Trans. Commun.*, vol. 39, no. 5, pp. 794–807, 1991.
- [40] P. Yegani and C. D. McGillem, "A statistical model for the factory radio channel," *IEEE Trans. Commun.*, vol. 39, no. 10, pp. 1445–1454, 1991.
- [41] H. Hashemi, "Impulse response modeling of indoor radio propagation channels," *IEEE J. Select. Areas Commun.*, vol. 11, no. 7, pp. 967–978, 1993.
- [42] G. A. Hufford, "A characterization of the multipath in the HDTV channel," *IEEE Trans. Broadcasting*, vol. 38, no. 4, pp. 252–254, 1992.
- [43] R. A. Dalke, G. A. Hufford, and R. L. Ketchum, "A digital simulation model for local multipoint and multichannel multipoint distribution services," NTIA/ITS, U.S. Dept. Commerce, Boulder, CO, NTIA Rep. 97-340, July 1997.
- [44] K. Pahlavan and S. J. Howard, "Statistical AR models for the frequency selective indoor radio channels," *Electron. Lett.*, vol. 26, no. 15, pp. 1133–1135, 1990.
- [45] W. C. Sabine, *Collected Papers on Acoustics*. New York: Dover, 1964.
- [46] E. Buckingham, "Theory and interpretation of experiments on the transmission of sound through partition walls," *Sci. Papers Bureau Standards*, vol. 20, pp. 193–219 and 1924–1926.
- [47] R. F. Norris, "Application of Norris–Andree method of reverberation measurement to measurements of sound absorption," *J. Acoustic. Soc.*, vol. 4, pp. 361–370, 1993.
- [48] R. W. Young, "Sabine reverberation equation and power calculations," *J. Acoustic. Soc. Amer.*, vol. 31, no. 7, pp. 912–921, 1959.
- [49] C. F. Eyring, "Reverberation time in DEAD rooms," *J. Acoustic. Soc.*, vol. 1, pp. 217–241, 1930.
- [50] P. M. Morse and R. H. Bolt, "Sound waves in rooms," *Rev. Mod. Phys.*, vol. 16, no. 2, pp. 69–150, 1944.
- [51] W. J. Sette, "A new reverberation time formula," *J. Acoustic. Soc.*, vol. 4, pp. 193–210, 1933.
- [52] G. Millington, "A modified formula for reverberation," *J. Acoustic. Soc.*, vol. 4, pp. 69–82, 1932.
- [53] L. E. Kinsler and A. R. Frey, *Fundamentals of Acoustics*, 2nd ed. New York: Wiley, 1962, ch. 14.
- [54] H. Kuttruff, *Room Acoustics*. Norfolk, U.K.: Applied Science, 1973, ch. 5.
- [55] A. D. Pierce, *Acoustics: An Introduction to its Physical Principles and Applications*. Woodbury, NY: Acoustic. Soc. Amer., 1989, ch. 6.
- [56] E. K. Dunens and R. F. Lambert, "Impulsive sound-level response statistics in a reverberant enclosure," *J. Acoust. Soc. Amer.*, vol. 61, no. 6, pp. 1524–1532, 1977.
- [57] E. T. Paris, "On the coefficient of sound-absorption measured by the reverberation method," *Phil. Mag.*, vol. 5, no. 29, pp. 489–487, 1928.
- [58] T. F. W. Embleton, "Absorption coefficients of surfaces calculated from decaying sound fields," *Acoustic. Soc. Amer.*, vol. 50, no. 3, pt. 2, pp. 801–811, 1970.
- [59] D. A. Hill, "Electronic mode stirring for reverberation chambers," *IEEE Trans. Electromag. Compat.*, vol. 36, no. 4, pp. 294–299, 1994.
- [60] B. H. Liu, D. C. Chang, and M. T. Ma, "Eigenmodes and the composite figure of merit of a reverberating chambers," Nat. Bureau Stand. Tech. Note 1066, Aug. 1983.
- [61] M. T. Ma, "Understanding reverberating chambers as an alternative facility for EMC testing," *J. Electromag. Wave Appl.*, vol. 2, nos. 3/4, pp. 339–351, 1988.
- [62] J. M. Dunn, "Local high-frequency analysis of the fields in a mode-stirred chamber," *IEEE Trans. Electromag. Compat.*, vol. 32, no. 1, pp. 53–58, 1990.
- [63] D. A. Hill, J. W. Adams, M. T. Ma, A. R. Ondrejka, M. L. Crawford, and R. T. Johnk, "Aperture excitation of electrically large, lossy cavities," Nat. Inst. Stand. Tech. Note 1361, Sept. 1993.
- [64] J. M. Ladbury, R. T. Johnk, and A. R. Ondrejka, "Rapid evaluation of mode-stirred chambers using impulsive waveforms," Nat. Inst. Stand. Tech. Note 1381, June 1996.
- [65] D. A. Hill, "A reflection coefficient derivation for the  $Q$  of a reverberation chamber," *IEEE Trans. Electromag. Compat.*, vol. 38, no. 4, pp. 591–592, 1996.
- [66] C. W. Kosten, "The mean free path in room acoustics," *Acustica*, vol. 10, pp. 245–250, 1960.
- [67] F. V. Hunt, "Remarks on the mean free path problem," *J. Acoustic. Soc. Amer.*, vol. 36, no. 3, pp. 556–564, 1964.
- [68] L. Batchelder, "Reciprocal of the mean free path," *J. Acoustic. Soc. Amer.*, vol. 36, no. 3, pp. 551–555, 1964.
- [69] R. R. DeLyser, C. L. Holloway, R. T. Johnk, A. R. Ondrejka, and M. Kanda, "Figure of merit for low frequency anechoic chambers based on absorber reflection coefficients," *IEEE Trans. Electromag. Compat.*, vol. 38, no. 4, pp. 576–584, 1996.
- [70] L. M. Brekhovskikh, *Waves in Layered Media*. New York: Academic, 1960, ch. 1.
- [71] C. A. Balanis, *Advanced Engineering Electromagnetics*. New York: Wiley, 1989, ch. 5.
- [72] K. S. Yee, "Numerical solution of initial boundary value problem involving Maxwell's equations in isotropic media," *IEEE Trans. Antennas Propag.*, vol. 14, pp. 302–307, 1966.
- [73] A. Taflov, *Computational Electrodynamics: The Finite-Difference Time-Domain Method*. Boston: Artech House, 1995.
- [74] J. P. Berenger, "A perfectly matched layer for the absorption of electromagnetic waves," *J. Computational Phys.*, vol. 114, pp. 185–200, 1994.
- [75] R. H. Espeland, E. J. Violette, and K. C. Allen, "Millimeter wave wide-band diagnostic probe measurements at 30.3 GHz on an 11.8 km link," NTIA Tech. Memo. TM-83-95, U.S. Dept. Commerce, Boulder, CO, Sept. 1983.
- [76] P. B. Papazian, Y. Lo, E. E. Pol, M. P. Roadifer, T. G. Hoople, and R. J. Achatz, "Wideband propagation measurements for wireless indoor communication," NTIA Rep. 93-292, U.S. Dept. Commerce, Boulder, CO, Jan. 1993.
- [77] W. B. Westphal and A. Sils, "Dielectric constant and loss data," Tech. Rep. AFML-TR-72-39, MIT, Cambridge, Apr. 1972.
- [78] K. Sato, H. Kozima, H. Masuzawa, T. Manabe, T. Ihara, Y. Kassas-hima, and K. Yamaki, "Measurements of reflection characteristics and refractive indices of interior construction material in millimeter-wave bands," in *1995 IEEE 45th Vehicular Technology Conf.*, Chicago, IL, 1995, pp. 449–453.
- [79] C. L. Holloway, P. L. Perini, R. R. DeLyser, and K. C. Allen, "Analysis of composite walls and their effects on short-path propagation modeling," *IEEE Trans. Veh. Technol.*, vol. 46, no. 3, pp. 730–738, 1997.
- [80] M. O. Al-Nuaimi and M. S. Ding, "Prediction models and measurements of microwave signals scattered from building," *IEEE Trans. Antennas Propag.*, vol. 42, no. 8, pp. 1126–1137, 1994.
- [81] W. Honcharenko and H. L. Bertoni, "Transmission and reflection characterization of concrete block walls in the UHF bands proposed for future PCS," *IEEE Trans. Antennas Propag.*, vol. 43, no. 2, pp. 232–239, 1994.
- [82] O. Landron, M. L. Feuerstein, and T. S. Rappaport, "A comparison of theoretical and empirical reflection coefficients for typical exterior wall surfaces in a mobile radio environment," *IEEE Trans. Antennas Propag.*, vol. 44, no. 3, pp. 341–351, 1996.



**Christopher L. Holloway** (S'86–M'92) was born in Chattanooga, TN, on March 26, 1962. He received the B.S. degree from the University of Tennessee at Chattanooga in 1986 and the M.S. and Ph.D. degrees from the University of Colorado at Boulder in 1988 and 1992, respectively, both in electrical engineering.

In 1992, he was a Research Scientist with Electro Magnetic Applications, Inc., Lakewood, CO. His responsibilities included theoretical analysis and FDTD modeling of various electromagnetic problems. From 1992 to 1994, he was with the National Center for Atmospheric Research (NCAR), Boulder. While at NCAR his duties included wave-propagation modeling, signal processing studies, and radar systems design. Since 1994, he has been with the Institute for Telecommunication Sciences (ITS) at the U.S. Department of Commerce, Boulder, where he is involved in wave-propagation studies. He is also a Consultant on the design of electromagnetic anechoic test chambers. His research interests include electromagnetic field theory, wave propagation, guided wave structures, remote sensing, numerical methods, and EMC/EMI issues.

Dr. Holloway is a member of Commission A of the International Union of Radio Science and is an Associate Editor on propagation for the IEEE TRANSACTIONS ON ELECTROMAGNETIC COMPATIBILITY.



**Michael G. Cotton** (M'98) received the B.S. degree in aerospace engineering in 1992 and the M.S. degree in electrical engineering with an emphasis on electromagnetics in 1999, both from the University of Colorado at Boulder.

In 1992, he joined the Radio Research and Standards Group at the Institute for Telecommunication Sciences, Boulder.

**Paul McKenna** (M'83) received the A.B. (astronomy) degree from Harvard University, Cambridge, MA, and the M.S. (astrogeophysics) degree from the University of Colorado at Boulder.

From 1982 to 1998, he was with Electro Magnetic Application, Inc., Lakewood, CO. His work there included time and frequency domain numerical solutions of Maxwell's equations in one, two, and three dimensions, with applications to HPM, EMP, SREMP, HIRF, EMC, EMI, and lightning coupling to systems and electromagnetic scattering from systems. In 1998, he joined the Institute for Telecommunication Sciences (ITS), U.S. Department of Commerce, Boulder, where he is involved in wave-propagation studies.

Mr. McKenna is a NARTE certified Engineer.